Natural Hazards (2026) 122:332
https://doi.org/10.1007/s11069-026-08063-3

ORIGINAL PAPER

Impact-based extreme-wave intensity scale for high-resolution coastal forecasting

Catalina Aguirre[1,2,3] · Mauricio Molina[1,9] · Sebastián Correa[1] · Daniela Manosalva[1] · Felipe Caselli[1] · Cristian Parra[4] · Sergio Bahamóndez[1,5] · Gonzalo Concha[6] · Angella Undurraga[6] · Alejandro de la Maza[6] · Sebastián Morales[7] · Vinka Marinkovic[8] · Gisela Irribarra[8]

Received: 12 August 2025 / Accepted: 19 February 2026 / Published online: 26 March 2026

Abstract
Extreme wave events are recurring meteorological and oceanographic hazards that have a significant impact on coastal regions, leading to infrastructure damage, beach erosion, and adverse effects on fisheries and port operations, resulting in substantial economic losses in Chile. In recent decades, both the frequency and intensity of extreme wave events have increased, and this trend is projected to continue due to climate change, making Chile's extensive coastline particularly vulnerable. In this context, having access to accurate and high-resolution coastal wave forecasting is crucial for coastal users and stakeholders involved in assessing and managing the risks associated with extreme wave events. Here, we present a high-resolution coastal wave forecasting system, which is validated using in situ measurements in Valparaíso Bay. Additionally, an impact-based extreme wave intensity scale has been developed to improve risk communication, support the issuance of official early warnings, and enhance emergency response. A five-category scale, derived from a qualitative analysis of historical impacts on beaches and coastal infrastructure, is fully integrated into the forecasting system. Video cameras have been installed to provide real-time broadcasts of the coastline, facilitating continuous monitoring of wave conditions and their impacts during extreme wave events. Furthermore, the information is disseminated through a dedicated public website and various social media platforms to effectively communicate warnings and promote preventive actions. Key national public institutions responsible for issuing warnings and managing emergencies participate in the information flow, thereby strengthening risk governance and public decision-making, and increasing confidence in the reliability of the coastal wave intensity forecasts.

Keywords Wind-waves coastal forecasting · Extreme events · Coastal impacts · Real-time monitoring

Extended author information available on the last page of the article

1 Introduction

Extreme wind waves can significantly affect usual maritime activities. Particularly in coastal regions, these events can cause infrastructure damage, overtopping, and coastal erosion, as well as reduce economic activities such as artisanal fisheries and port operations (e.g., Koks et al. 2022; Heck et al. 2021; Camus et al. 2019; Ruggiero et al. 2001). As recurring meteorological and oceanographic (metocean) hazards, they demand operational forecasting and risk management efforts. Notably, extreme wave events have become more frequent and intense in recent decades. Research using satellite altimetry data to estimate trends in wave height has shown a significant increase in large areas of the oceans. Moreover, the rate of increase is higher and more extended for extreme wave heights compared to mean wave height conditions (Young and Ribal 2019), with significant positive trends observed throughout the entire Southern Hemisphere. However, there is substantial spatial variability, with the most significant increase in extreme wave heights in the Southern Ocean, consistent with the increment in extreme surface winds (Young et al. 2011). Furthermore, this wave-climate change pattern is expected to persist throughout the twenty-first century in the context of ongoing anthropogenic climate change (Hemer et al. 2013; Morim et al. 2018; Meucci et al. 2020).

Due to the prominent meridional extent of the Chilean coast (~4200 km), its wave climate is strongly influenced by the latitudinal variation of mean surface wind speed, where the stronger winds over the Southern Ocean play a significant role in generating higher waves at higher latitudes (e.g., Aguirre et al. 2017). Intense fetches, typically associated with extratropical cyclones (low-pressure cores), serve as the energy sources of extreme wave events along the coasts of Chile. During the austral winter, the track density of extratropical cyclones displaces northward, forming extreme wave events at lower latitudes. These cyclones could generate powerful winter surges that impact the coast (e.g., Winckler et al. 2017). During austral summer, extreme waves generated by boreal winter storms in the North Pacific spread as long swells toward the Southeast Pacific (Winckler et al. 2025; Aguirre et al. 2020). In Chile, the average number of wave-extreme events is 40 per year, however, in the last 40 years, they have increased, with 1 to 3 more events per decade, depending on latitude (Winckler et al. 2020). Exceptional wave-extreme events have caused significant damage to the coastal zone, as seen on August 8, 2015 (Winckler et al. 2017), which was cataloged as a meteotsunami (Carvajal et al. 2017), and in island locations (Carvajal et al. 2021). Extreme wave events have led to coastal erosion, infrastructure damage, and impacts on wetlands, port operations, and marine communities. For example, Martinez et al. (2022) studied 45 sandy beaches covering nearly 2000 km along the Chilean coast. Their results show that 80% of the sites present erosion rates, attributing this generalized shoreline retreat partly to an increase in the frequency of extreme wave events (Martinez et al. 2018). Furthermore, erosion feedback and the projected sea-level rise exacerbate the impacts of extreme wave events along the Chilean coast (Albrecht & Shaffer 2016).

Impacts produced by extreme wave events vary and affect socioeconomic activities at different scales, ranging from suspending recreational pastimes on the coast to destroying infrastructure and even resulting in loss of human life. In fact, the World Meteorological Organization (WMO) advocates for the development of early warning systems that protect citizens from extreme events in the short term, thereby advancing climate change adaptation. By identifying approaching hazards as early as possible, communities can prepare in

advance and minimize disturbance and damage (WMO 2022). According to the special report on managing the risk of extreme events by the Intergovernmental Panel on Climate Change (IPCC), to be effective and complete, an early warning system is typically composed of four interacting elements: 1) generation of risk knowledge, including monitoring and forecasting, 2) surveillance and warning services, 3) dissemination and communication, and 4) response capability. Warnings are received and understood by the target audience and are most relevant when the communication has a shared meaning between those who issue the forecasts, possess local knowledge, and the decision-makers they are intended to inform (IPCC 2012). In Chile, the official early warnings of extreme wave events issued by the Meteorological Service of the Navy (SERVIMET) still have a macro-regional spatial resolution and are updated daily. However, in the coastal region, it is possible to find very different wave conditions just a few kilometers away. Such variability is primarily caused by changes in bathymetry and coastline configuration, which can generate wave shadows and alter wave propagation, particularly affecting wave height and direction (Fig. 1). Nevertheless, several freely available global wave forecasts also miss the detailed coastal features due to their coarse spatial resolution and thus fail to simulate coastal wave conditions. Bridging this scale gap is therefore critical for effective risk assessment and local decision-making.

In this work, we validate a high-resolution coastal wave forecasting system implemented in Valparaíso Bay, central Chile. Furthermore, a qualitative extreme-wave intensity scale is proposed and integrated into the wave forecasting system, translating information into likely impacts that are understandable to the general public without requiring technical wave knowledge. This approach helps risk communication by converting technical wave parameters into actionable warnings. Thus, we support institutions that interact for an effective early-warning system, as our workflow operationalizes hazard knowledge through continuous coastal monitoring, a high-resolution wave forecasting system, and communication to SERVIMET, the National Service for Disaster Prevention and Response (SENAPRED), and the National Fisheries and Aquaculture Service (SERNAPESCA). This institutional con-

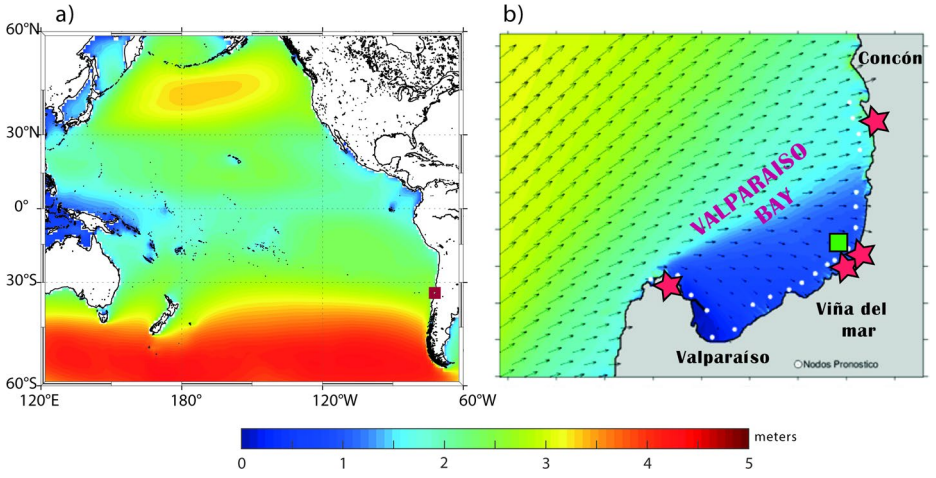

Fig. 1 Study Area. **a** The model domain used for forecasting and the average significant wave height (m) derived from wave-model data. **b** Valparaíso Bay: white dots indicate coastal nodes for high-resolution forecasting, the green square shows the location of wave measurements, and red stars mark the locations of cameras monitoring the coastal area

nection has facilitated cooperative discussions, making the tool usable for national public services, improving access to hazard information, and strengthening community preparedness. Additionally, public dissemination of results is facilitated by an open-access webpage at www.marejadas.uv.cl and social media updates.

2 Methods

2.1 Wave forecasting system

The model used to generate the wave forecast is the Wavewatch III version 4.18b, a third-generation spectral wind-wave model developed by the National Centers for Environmental Prediction (NCEP) of the National Weather Service of the United States (Tolman, 2014). We simulate the Pacific Ocean basin, spanning from 110°E to 299°E in longitude and from 64°N to 64°S in latitude, with a spatial resolution of $1° \times 1°$. To generate the grid, we implemented the automated grid generation tools for Wavewatch III (Chawla & Tolman 2007), which uses bathymetry from the General Bathymetric Chart of the Oceans (GEBCO) with a one-arc-minute grid resolution. The shoreline data used is the Global Self-Consistent Hierarchical High-Resolution Shoreline (GSHHS) with a resolution of 40 m. To force the model, we use wind fields 10 m above the sea surface with a temporal resolution of 3 h and a spatial resolution of 0.5° from the Global Forecast System (GFS), which is generated from a coupled atmosphere, ocean circulation, land surface, and sea ice model to represent weather conditions (e.g., NCEP, 2004).

The wave model spectral domain was discretized into 29 frequencies, ranging from 0.0345 Hz to 0.4975 Hz, with an increment factor of 1.1, and 24 regularly spaced directions (15° intervals). Parametrizations used include the following: (1) the ST4 source term package (Ardhuin et al. 2010), (2) the Discrete Interaction Approximation (DIA) to simulate nonlinear wave-wave interactions (Hasselmann et al. 1985), and (3) the third-order Ultimate Quickest (UQ) propagation scheme along with the averaging technique (PR3) for alleviating the Garden Sprinkler Effect (Tolman 2002). Using this configuration, a 7-day forecast has been operational since 2017 and remains so to the present day. Gridded significant wave height (SWH), mean and peak wave period (T_m and T_p), and mean and peak wave direction (D_m and D_p), and 79 points with spectral data in deep water along the coast and surrounding Chilean islands are saved hourly (Correa et al. 2025).

The model used to generate the high-resolution coastal wave forecast is the Simulating Waves Nearshore (SWAN) version 41.45, a third-generation wave model developed at Delft University of Technology (Holthuijsen et al. 1993). The Valparaíso Bay domain extends from 70.5°W to 71.8°W in longitude and from 32.8°S to 33.1°S in latitude. Simulations are performed on an unstructured grid with horizontal resolution ranging from 2 km offshore to 25 m near the coast, comprising a total of 6,491 nodes. The bathymetry for the coastal region is derived using three nautical charts provided by the Hydrographic and Oceanographic Service of the Chilean Navy (SHOA), covering regional to local scales (Table 1). Data from nautical charts and GEBCO are processed in OceanMesh2D (Roberts et al. 2019) to refine coastal bathymetry.

The spectral wave energy transfer to the shallow waters of Valparaíso Bay is based on the unit spectrum propagation method (e.g., Dominguez et al. 2014). This approach con-

Table 1 Information about the nautical charts used to construct the coastal bathymetry

Number	Name	Scale
5000	Bahía Valparaíso a Golfo de Arauco	1:500,000
5100	Punta Pite a Punta Topocalma y puertos adyacentes	1:200,000
5111	Bahía y puerto Valparaíso	1:10,000

sists of generating synthetic spectra with a significant wave height of 1 m for different frequency–direction pairs. These spectra are then propagated independently using the SWAN wave model, and the resulting output spectra are used to construct a transfer function. This function is subsequently applied to the real offshore spectrum to obtain the equivalent transformed spectra at the site of interest. Consequently, the transformation process using this transfer function requires relatively low computational cost and time.

The astronomical tides are obtained through the Fourier series analysis methodology (Pawlowicz et al. 2002) using the sea level data from a tide gauge located off Valparaíso at -33.03ºS and -71.63ºW maintained by SHOA and available at https://www.ioc-sealevelmonitoring.org. We generate astronomically driven sea-level forecasting using more than forty tidal harmonics. Since sea level variability may be important, the wave energy transfer process to shallow water is carried out for high and low tide conditions. Once the deep-water spectra and the tide are forecasted, the propagation method is applied by linearly interpolating the energy transfer coefficients according to the sea level. Thus, we obtain the wave spectra with high spatial resolution along the coast and calculate wave parameters (H_s, T_m, T_p, T_e, D_m, and D_p). Using H_s and T_p the wave energy flux (EF) is calculated as $EF = 0.49H_s^2T_p$. Furthermore, the high-resolution coastal wave forecast, along with the sea-level forecast and coastline features, allows the evaluation of some processes at the sea-land interface, such as run-up and overtopping discharge. The normalized vertical run-up excursion is calculated following Guza et al. (1984)

$$\frac{R}{H_s} = \begin{cases} \left(\frac{\pi}{2\beta}\right)^{1/2} : \xi_0 \geq \xi_c \\ \frac{\xi_0^2}{\pi} : \xi_0 < \xi_c \end{cases}$$

$$\xi_0 = \frac{tan\beta}{(H_s/L_0)^{1/2}}; \xi_c = \left(\frac{\pi^3}{2\beta}\right)^{1/4}$$

where ξ_0 is the Iribarren number, a nondimensional surf similarity parameter useful in parameterizing several surf zone processes, and ξ_c is an expression for the condition at which the transition between non-breaking and breaking occurs (Iribarren and Nogales, 1949; Battjes, 1974). β is the beach slope and L_0 is the deep water wave length $L_0 = gT^2/2\pi$. To calculate the mean discharge overtopping (q), we follow the design method of Owen (1980)

$$\frac{q}{T_m g H_s} = Q_0 exp\left(-b\frac{R_c}{T_m\sqrt{gH_s}}\right)$$

where g is the acceleration due to gravity, *Rc* is the freeboard (modulated by tides), and Q_0 and b are empirically derived coefficients which depend on the profile of the coastal structure.

2.2 Forecast validation

To evaluate the performance of the coastal high-resolution forecasting, we compare results with measurements using an Acoustic Doppler Current Profiler (ADCP) Signature 1000 installed in the Valparaíso Bay at 33º00' S; 71º33' W. Data from December 2021 to December 2022 are obtained in three distinct periods detailed in Table 2. Statistical error metrics such as bias, root mean squared error (RMSE), and temporal linear correlation (R) are used to assess the difference between the observed and forecasted wave data. This statistical analysis was performed using hourly time series. The formulations of these error metrics are

$$bias = \frac{1}{N}\sum_{i=1}^{N} P_i - O_i$$

$$RMSE = \sqrt{\frac{1}{N}\sum_{i=1}^{N}\left[\left(P_i - \overline{P}\right) - \left(O_i - \overline{O}\right)\right]^2}$$

$$R = \frac{\sum_{i=1}^{N}\left(P_i - \overline{P}\right)\left(O_i - \overline{O}\right)}{\sqrt{\sum_{i=1}^{N}\left(P_i - \overline{P}\right)^2 \sum_{i=1}^{N}\left(O_i - \overline{O}\right)^2}}$$

N is the data length, P_i is the predicted data, and O_i is the observed data.

Also, we compare the performance of the coastal high-resolution forecasting system implemented at Valparaíso Bay, with the results of other freely available global wave forecasts, such as Wisuki, Windguru, Windy, and Windfinder. The same error metrics are used for 40-day data.

Sea level data measured with the gauge pressure sensor from the ADCP are compared with the forecasted tide for one month. The geographical locations of the instruments and the measurement periods are indicated in Table 2 and shown in Fig. 1.

2.3 Intensity scale

The first step in creating an intensity scale for extreme wave events was to develop a detailed catalog based on the scope of their occurrence (Table 3). The impacts analyzed in this work occur in the two main coastal typologies present in Valparaíso Bay: beaches with adjacent structures (urban beaches) and breakwaters with coastal walkways. Here, extreme

Table 2 Information about the ADCP Measurements

Latitude	Longitude	Start date	End date	Length of data
33º00' S	71º33'W	17/12/2021	24/03/2022	2320
		04/04/2022	17/08/2022	2519
		25/09/2022	30/12/2022	2250

Table 3 Details of the scope of impact of extreme wave events on the coastal zone in Valparaíso Bay

	Scope of impacts	Type	Coastal tipology
A	Submerged activities and/or in coastal waters	Activity	
B	Shore activities in wet areas	Activity	Beach with a rear structure and coastal promenade
C	Beach activities in usually dry areas	Activity	
D	Run Up	Phenomena	
E	Beach Erosion	Phenomena	
F	Mobile elements	Furniture	
G	Buildings on the beach	Infrastructure	
H	Beach end protection structures	Infrastructure	
I	Buildings in protective structure	Infrastructure	
J	Overtopping	Phenomena	Breakwater with a coastal promenade
K	Pedestrian traffic	Activity	
L	Vehicular traffic	Activity	
M	Mobile elements	Furniture	
N	Coastal protection structures	Infrastructure	
O	Buildings close to coastal walks	Infrastructure	

Table 4 Simultaneous occurrence of impacts in the catalog

	Minor impact Major impact Severe impact	Impacts Catalog															category
			Beaches								Breakwater						
		A	B	C	D	E	F	G	H	I	J	K	L	M	N	O	
Waves	All null																N
																	N+
Extreme waves																	M1
																	M2
																	M3
																	M4
	All severe																M5

wave events can cause overtopping and strong run-up, damaging socioeconomic activities, including shore fishing, diving, and beach sports, as well as infrastructure and furniture, and can lead to beach erosion.

The selected scopes are divided into three levels of impact: 1) minor, 2) major, and 3) severe, as presented in the supplementary material (Table S1–S5) for different types of coastal zones. The catalog of impacts is then organized to classify those that co-occur within a single coastal typology and across multiple coastal typologies. The classification begins with a level where all impacts are null and progresses to a level where all impacts are severe, as detailed in Table 4.

Including the all-null impact level, we identified seven subdivisions representing the various categories associated with coastal waves. The initial level, characterized by the absence of any impact, corresponds to normal wave conditions, as there are no disruptions to activities typically carried out in the coastal zone. The next level accounts for only minor impacts on submerged activities, serving as a transitional stage between normal and extreme condi-

tions. The subsequent level represents the first category of extreme wave conditions (M1), where the impact on submerged activities becomes significant and initial effects on shore activities emerge. Furthermore, it is considered a key descriptor of extreme events when the run-up exceeds its usual boundaries and the first signs of beach erosion are observed. The following levels—M2, M3, and M4—depict the progressive intensification of impacts across all areas, including beaches and breakwater structures. Infrastructure damage begins at category M3. Finally, the highest level (M5) signifies a severe impact in all dimensions, representing the worst-case scenario.

The categories are defined based on the local wave climate at each location and are established using statistical parameters such as percentiles and return periods of 2, 5, and 25 years (RP2, RP5, and RP25, respectively) of *Hs*, wave energy flux, run-up, and overtopping discharge. An extreme wave event is classified into a given category when at least one variable exceeds the corresponding threshold. Table 5 presents a general qualitative description of each category's impact, aimed at enhancing the public's understanding, as well as the thresholds defined for each category. Designed for web page and social media diffusion purposes, Fig. 2 explicitly describes the limits of safe permanence on the coast for each category in both the beach configuration and the coastal walk with breakwater.

Table 5 General description of impacts by category for public understanding (Table in Spanish in supplementary Fig. S6)

	Category	Description	Thereshold
Waves	N	Usual activities are carried out. The restrictions are the usual ones.	$<75^{th}$
	N+	Usual activities in the water are carried out with difficulty but do not affect activities on shore or land. There are more restrictions on access to water than usual.	$75^{th} – 95^{th}$
Extreme wave events	M1	Entering the sea is dangerous; caution must be taken during shore activities. Water occasionally comes out on beaches.	$95^{th} – 99^{th}$
	M2	Carrying out coastal activities is dangerous. Beaches are frequently flooded, and sand erosion occurs. Water occasionally and, to a low extent, overflows the structures.	99^{th} – RP2
	M3	Approaching the wet area is dangerous. Beaches have erosion close to the annual maximum, coastal walks have frequent overtopping, generating minor flooding, and damage occurs to fragile structures.	RP2 – RP5
	M4	Coastal evacuation is suggested. Beaches are eroded more than usual, permanent structures are damaged, water leaves the beach boundaries, and properties are flooded.	RP5 – RP25
	M5	Coastal evacuation is necessary. Structures are severely damaged or destroyed; persistent overflows generate flows on coastal walks and streets and significant property damage or destruction.	>RP25

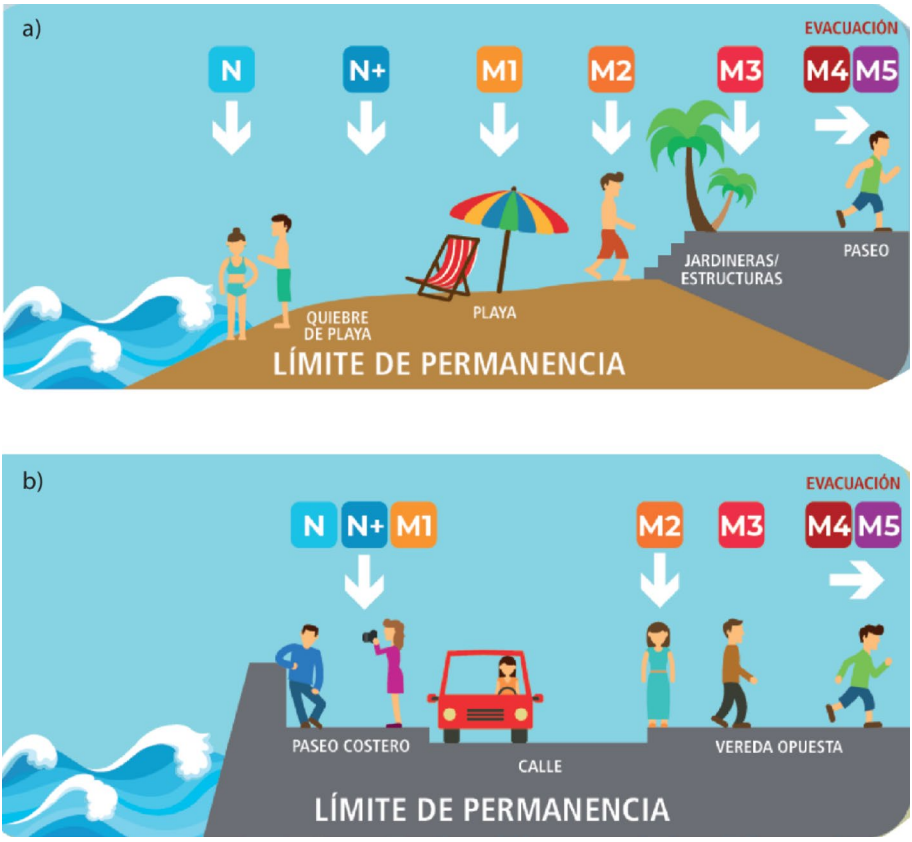

Fig. 2 Safety limit for stay. Outlines safe occupancy boundaries along the Bay for each category of extreme wave events, intended for community communication. **a** Beach configuration and **b** coastal walk with breakwater

3 Results

3.1 Forecast skill and comparative performance

Observed and forecasted wave parameters time series, heat scatter plots, and statistical error metrics are presented in this section to assess the skill of the operational coastal wave forecasting system. Generally, the comparison between wave forecast data and measurements shows good agreement for SWH variability. However, the model still underestimates Hs peak values, particularly in the winter season (Fig. 3). Negative bias values indicate that forecasted Hs data is underestimated relative to in situ measurements, and consistently, the heat scatter shows a systematic deviation below the 1:1 line at higher Hs values. Particularly during the austral winter, when extreme wave events increase in frequency, negative bias (RMSE) in forecasted Hs data increases its value to 0.14 m (0.21 m). In contrast, negative bias (RMSE) reduces to 0.09 m (0.13 m) and 0.01 m (0.12 m) during spring and summer, respectively. The correlation coefficient ranges from 0.59 to 0.87, with higher values observed during winter. This seasonal partitioning of the statistics highlights that model

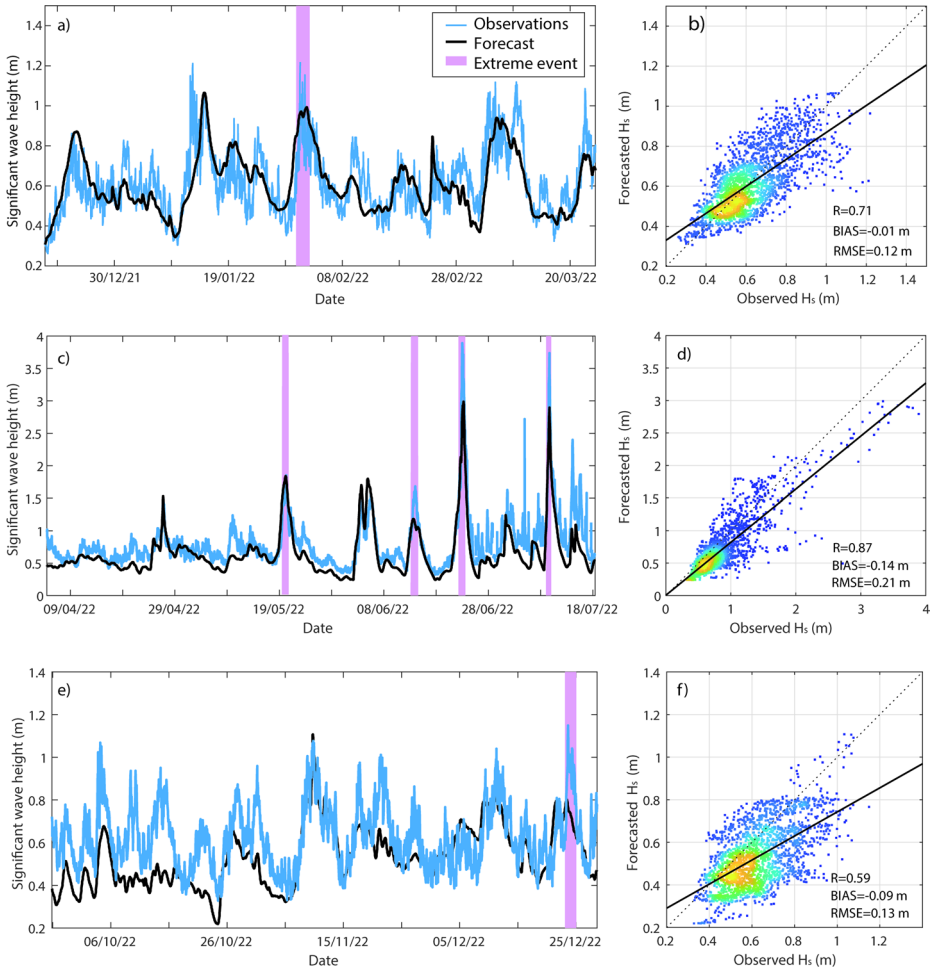

Fig. 3 Significant wave height validation. Time series and density scatter plot of observed versus forecasted significant wave height

skill decreases slightly under more energetic conditions but remains within acceptable performance for operational use. Although overall model performance is satisfactory, reduced skill is observed in reproducing the highest wave heights, consistent with previous evaluations of spectral wave models (e.g., Stopa et al. 2014). Lower performance for extreme events compared to the mean wave climate has also been documented along the Chilean coast (Beyá et al. 2017; Gallardo et al. 2017). This limitation is primarily associated with uncertainties in atmospheric forcing (Morim et al. 2023); however, it also reflects the still largely empirical nature of spectral wave models and the incomplete representation of some physical processes, which limits their ability to accurately simulate extreme conditions (Cavaleri et al. 2007).

Observed and forecasted T_p time series, heat scatter plots, and error metrics are shown in Fig. 4. The evolution of T_p at the measurement site demonstrates that the forecast accurately

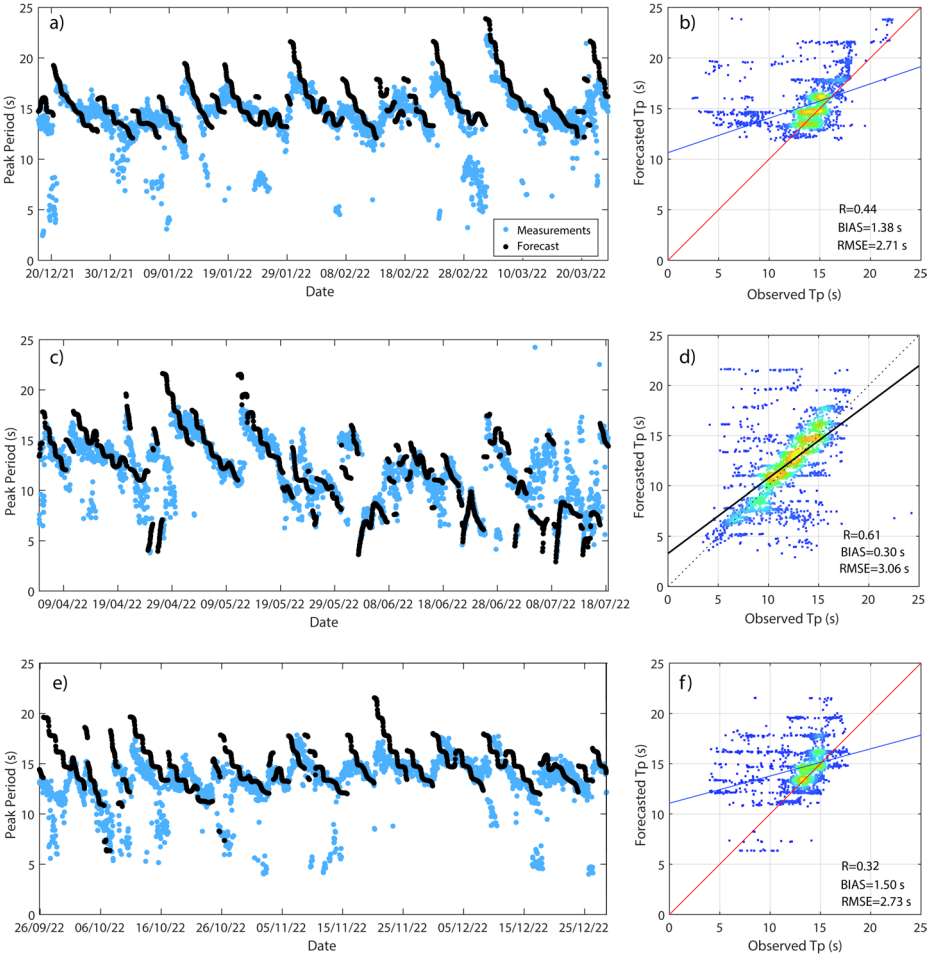

Fig. 4 Peak period validation. Time series and density scatter plot of observed versus forecasted wave peak period

captures the synoptic modulation of sea state and the timing of individual peaks. The model demonstrates a reasonable agreement with T_p observations, showing a positive bias —that is, an overestimation—of up to 1.5 s in winter, compared to 0.3 s in summer. This is consistent with previous research, which has found that wave models systematically overestimate the T_p as a result of longer wave period predictions in the Southern Ocean (Liu et al. 2021; Liu et al. 2022; Correa et al. 2025), significantly influencing the wave simulation in the Southeast Pacific, as the Southern Ocean swell predominates (Beyá et al. 2016; Aguirre et al. 2017). The RMSE also exhibits higher values during winter (RMSE = 3.1 s) and similar values during spring and summer (RMSE = 2.7 s). The correlation coefficient ranges from 0.32 to 0.61, with higher values observed during the winter months, respectively. These correlations are lower than those for Hs, given that T_p is more sensitive to mixed-sea states.

Time series of the forecasted Hs using different datasets are compared with observations recorded by the ADCP located in Valparaíso Bay (Fig. 5a), displaying concurrent Hs

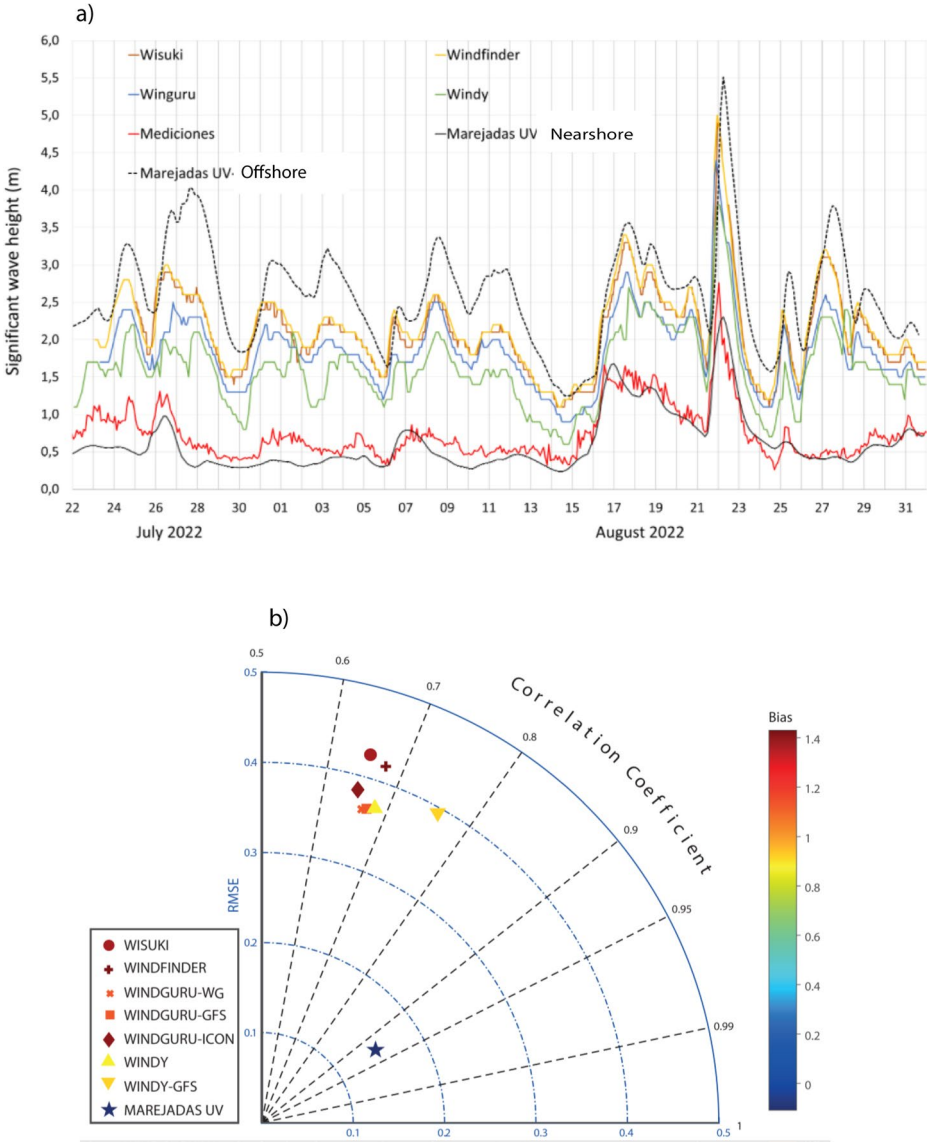

Fig. 5 Significant wave height comparison. **a** Time series of significant wave height at Valparaíso Bay from freely available global forecasting. **b** Error metrics diagram using observed significant wave height data from the ADCP and different freely available global forecasts

from the Pacific Ocean low-resolution forecast system (offshore), the coastal high-resolution system (nearshore), and several freely available global products (Wisuki, Windfinder, Windguru, Windy). The comparison shows that our coastal high-resolution forecast outperforms other freely available global forecast systems, which tend to overestimate in situ wave height measurements at the coast. This systematic overestimation is consistent with the coarse spatial resolution of global models and their limited representation of nearshore

wave transformation, which occurs due to refraction, shoaling, and shadowing resulting from local bathymetry and coastline geometry. For example, during the selected period, the buoy recorded an extreme wave event centered on August 22, 2022. Throughout this event, the maximum Hs values reached by global forecasts range between 3.8 m and 5 m, while the coastal forecasted Hs exhibits values of 2.6 m, which is much closer to the Hs value measured that day by the ADCP (2.3 m). Consequently, the bias of our coastal forecast (~0.3 m) is markedly smaller than that of the global models (~1.5–2.7 m) for this specific event; however, it highlights the important systematic positive bias when using global models to forecast Hs in the coastal region.

To visualize the behavior of the different statistical error metrics obtained for each dataset—namely, bias, RMSE, and R —a diagram is presented in Fig. 5b. Specifically, it is a modified Taylor diagram in which the radial distance represents RMSE, the arc indicates R, and the color encodes the mean bias. Most Hs data freely available from global low-resolution models exhibit similar correlation and RMSE values in the global forecasting data, with their markers clustering around 0.40 m RMSE and the R values ranging from 0.65 to 0.70. Windy-GFS shows a better correlation, with R values of 0.76; however, its RMSE remains comparable to that of the other global products. The bias exhibits positive values of Hs, with overestimation as high as 0.8 m to 1.5 m in global products. In contrast, a significantly lower bias value is found when the observed data are compared with our high-resolution coastal forecasting system, whose point lies closest to the origin, quantitatively confirming its superior skill for coastal applications.

The comparison of forecasted astronomical tides with sea-level measurements yields precise results, with an R-squared value of 0.99 and an RMSE of 0.06 m (Fig. 6). Data points cluster tightly along the 1:1 line (Fig. 6b). This demonstrates that astronomical tide forecasting can accurately represent sea-level variations in the coastal region, despite being influenced by various processes and factors beyond the tide, such as meteorological forcing and wave setup, among others. Overall, the wave and tide forecast skill supports operational use providing the technical basis for the impact-based coastal product described next.

3.2 Impact-based coastal forecast

The extreme wave intensity scale has been implemented in the high-resolution coastal wave forecasting system for the Valparaíso Bay. The information is presented as a mosaic of wave intensity categories (Fig. 7), which on the vertical axis describes the coastal locations considered in the forecast, and the horizontal axis presents the next 7 days with an hourly

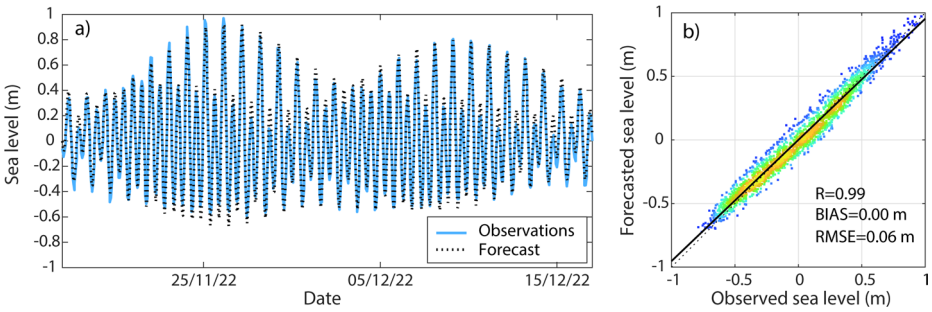

Fig. 6 Sea level validation. Time series and density scatter plot of observed versus forecasted sea level

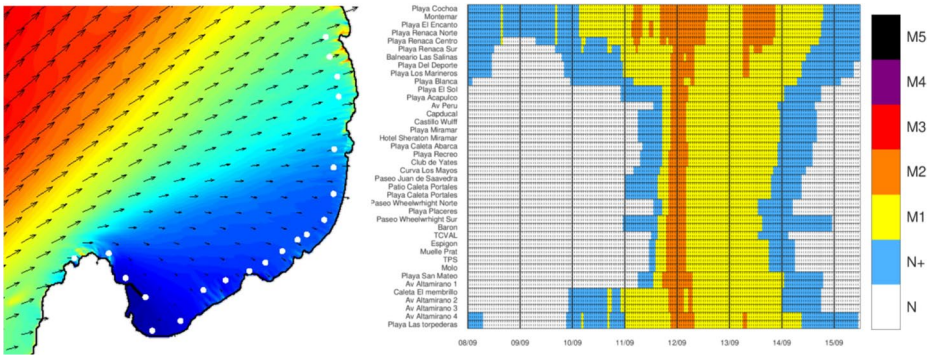

Fig. 7 Mosaic. Example of visualization of the high-resolution wave intensity forecast in Valparaíso Bay

temporal resolution. Each cell, therefore, represents a unique space–time bin and is colored according to the five-category scale evaluating the coastal wave and tide forecasted conditions. The sea level variability associated with astronomical tides can modulate transitions between distinct categories, particularly if an extreme wave event occurs during a spring tide period. In this way, we increase the spatial resolution of macro zones (administrative regions in Chile) to microzones within the Valparaíso Bay, and make a transition from a public forecast of wave parameters to their expected impacts on the coast at hourly temporal resolution. This enables the rapid identification of stripes of elevated impact and highlights alongshore heterogeneity within the Bay, serving as an operational tool to support short-term decision-making, allowing national agencies and coastal users to prioritize locations and time windows with higher expected impacts.

The complete mosaic for the operational period of the wave forecasting system is shown in Supplementary Fig. S7, illustrating the higher frequency and intensity of extreme wave events during winter, whereas summer events tend to be longer-lasting and strongly modulated by tidal conditions. These summer events are typically associated with swell generated in the Northern Hemisphere that propagates across the Pacific Ocean and reaches the Chilean coast with long wave periods due to frequency dispersion. A qualitative evaluation of the impact-based wave scale was conducted using information from press reports, social media records, and coastal monitoring cameras. These sources enabled an assessment of the observed impacts of extreme wave events. The complete list of extreme wave events considered in this analysis is provided in Supplementary Table S8. All M4-category events and most M3-category events identified in the forecast were also observed in the reported impacts; however, some M3 events did not show documented impacts when they affected only a limited area within the bay. In addition, several M1- and M2-category events were forecast, although impacts could not be identified for all of them, as these events generally do not produce sufficiently severe or newsworthy consequences. During the operational period of the wave forecasting system, no M5-category events have been forecasted.

3.3 Real-time monitoring, operational workflow, and dissemination pathways

Since the 2022 wave impact monitoring has been implemented in Valparaíso Bay by installing IP cameras at four locations on the coastline: Reñaca Beach, Acapulco Beach, Av. Perú

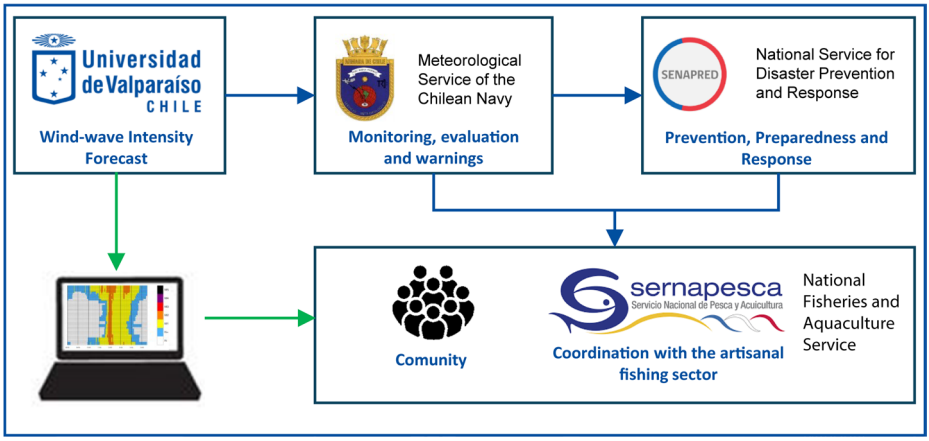

Fig. 8 Transfer of information. Diagram of the flow of information from the wave intensity forecast to the community and public institutions

(coastal walkway), and Las Torpederas Beach. The images from the four cameras are being also transmitted in real-time through the YouTube channel @MarejadasUV (https://www.youtube.com/@MarejadasUV). Authorities typically utilize this relevant information during extreme wave events to support near-real-time risk assessment and response coordination. TV news also utilizes our transmission to inform the population, and people can access our YouTube channel directly, with 8.6 k subscriptions and over one million total views to date. The live-stream audience effectively constitutes an auxiliary observation network. User-generated, time-stamped comments frequently mark the initial occurrence of overtopping, providing opportunistic real-time ground truth that enhances situational awareness and supports risk communication. As expected, channel analytics show step changes in views and subscriptions coinciding with extreme-wave events, indicating heightened engagement and information demand. In fact, typical peak event audiences are approximately 1.5 to 2 k concurrent users.

The massification model of high-resolution wave intensity forecasting is based on communicating the information generated between the relevant stakeholders involved when an extreme wave event develops. Operationally, this functions as an information dissemination and risk governance workflow. First, results enable us to achieve high precision in coastal wave forecasting, which is incorporated as one of the primary sources of information used by SERVIMET to issue official warnings for extreme wave events. Figure 8 illustrates the information flow, where the University of Valparaíso generates a coastal wave intensity forecast for the next seven days and sends it daily at 6:30 am local time to SERVIMET. SERVIMET, if the case, issues official extreme wave event warnings for public institutions and coastal users as needed. Thus, this key technical entity has additional high-resolution input for monitoring and evaluation. When forecast thresholds indicate the destructive potential of an extreme wave event, the alert is escalated to the SENAPRED for prevention, preparedness, and response actions. Additionally, the information is targeted at the artisanal fishing sector through support from the National Fisheries and Aquaculture Service (SERNAPESCA), facilitating communication with fishermen and mitigating the negative

impacts on this economic activity. In summary, the workflow formalizes the forecasting, warning, and emergency management chain with key national institutions.

The forecast information is also available on the website www.marejadas.uv.cl, whose visitor numbers have increased significantly over time. As in YouTube channel, the website shows increase in traffic coincident with extreme-wave episodes, consistent with amplified information demand during hazard onset and evolution. Notably, approximately 15% of the website's visits are from abroad. The web interface displays the Pacific Ocean Hs forecast and local hourly wave parameters, as well as the 7-day intensity forecast matrix, described in Fig. 7. This allows users to select specific locations along the coast and visualize the evolution between distinct intensity categories of extreme wave events. Furthermore, on this website, users can register free of charge to obtain high-resolution wave intensity forecasts for extreme wave events in a specific coastal location, if available. Once the user registers, they receive daily high-resolution forecast information by email. Currently, 180 registered users receive personalized impact forecast information daily. This subscription service formalizes risk communication to coastal users by providing a standardized information structure.

Social media has also been essential in disseminating our coastal high-resolution wave intensity forecasting, thanks to its massive reach and speed of transmission, which allows information to quickly influence coastal communities, fishermen, and tourists who may be affected by an extreme wave event. In fact, the high use of social media by the population reduces the latency of warning dissemination and amplifies reach through network effects, enabling the rapid propagation of official updates during extreme wave periods. This strengthens prevention and mitigates risks by ensuring that more people are informed and have sufficient time to act and mitigate impacts. Currently, we have the following direct users across social media: 7,1 K followers on Instagram, 2,4 K followers on X (formerly Twitter), and 1,6 K followers on Facebook. Consistent with the website and YouTube channel, the social media exhibit step changes in followers and views during extreme wave events, indicating increased engagement at times when actionable forecasts and real-time information are most needed.

4 Summary and future work

We have presented a high-resolution coastal wave forecasting system for the Valparaíso Bay, which is currently operational at the University of Valparaíso. The forecast data have been successfully validated using in-situ wave information recorded by ADCP and exhibit the highest level of reliability in coastal areas compared to other freely available global wave forecasts, such as Wisuki, Windguru, Windy, and Windfinder. This added value arises from resolving nearshore wave transformation driven by bathymetry and shoreline geometry, and is reflected in significantly lower bias and RMSE, as well as higher correlation for Hs at the coast. Thus, the results provide the most precise public tool for forecasting extreme wave events along the Chilean coast among the other products evaluated in this study.

Additionally, we proposed an intensity scale for extreme wave events based on a qualitative analysis of their impact when reaching the coastline, such as overtopping, run-up, and beach erosion. The scale has five levels or categories, designed to make it easier for coastal users to understand by using a numerical scale that feels intuitive. Operationally, categories

are assigned based on combined thresholds in Hs, Tp, and tidal level, evaluated hourly at micro-zone locations. This method helps coastal users better understand the severity of wave impacts. It also allows for distinguishing between destructive and non-destructive events, providing insights into the gradual effects on coastal activities, potential damage to infrastructure, evacuation needs, and the frequency of these events. In practice, categories highlight windows of time and location with increased expected impacts, aiding in preventive measures, resource allocation, and coordination with emergency services. As a result, coastal users can take appropriate actions based on the severity of an impending extreme wave event, and agencies can coordinate warnings and responses more effectively.

To share information on coastal wave intensity forecasting, collaboration has been established with key public institutions mandated by law to issue official extreme wave event warnings (SERVIMET) and disaster prevention and management (SENAPRED). This partnership formalizes the coastal high-resolution forecast to support the issuance of early warnings and strengthen the response chain. It represents a collective, multi-agency effort to reduce risks, share experience, and coordinate stakeholders to improve governance and institutional capabilities as extreme wave events become more frequent due to a warming climate. Additionally, SERNAPESCA serves as a link to the artisanal fisheries, enhancing communication and preparedness within this sector. The importance of involved public institutions enables direct and indirect access for many users. However, a dedicated website and social media platforms are also used to distribute the information generated by the coastal wave intensity forecasting system.

Although high-resolution coastal forecasting and coastline monitoring have recently focused on Valparaíso Bay, their results will be expanded to cover the entire country facing the Pacific Ocean in the coming years. Several new cameras will be installed along the Chilean coastline, and specialized photogrammetry techniques will be employed to determine the position of the coastline relative to the camera locations, georeferenced points within the images, and the exact time of image capture, following algorithms such as CoastSnap (e.g., Harley and Kinsela 2022). All this information will allow us to create structured and georeferenced databases that utilize artificial intelligence to validate the intensity scale and continually enhance the performance of extreme wave event impact forecasting along the coast (e.g., bias correction, nowcasting of category transitions), which will be a focus in the future. Particularly, the lower categories can be validated for robustness using a quantitative assessment of impacts.

In future upgrades of coastal wave forecasting, there will be a focus on testing and implementing coupled regional models that integrate wave dynamics with other physical processes, such as atmospheric and surface ocean circulation. This includes atmosphere–wave–ocean coupling with wave–current–wind feedbacks (e.g., Stokes drift and current-induced refraction), as well as evaluating storm surge conditions. Previous preliminary coupling efforts have been conducted on the Chilean coast in hindcast mode, considering interactions and feedback processes between surface winds, currents, and waves (Bahamóndez & Aguirre 2023). We will expand this effort to develop a comprehensive coastal forecasting system that incorporates new ocean and atmospheric variables, providing accurate coastal forecast information to support informed decision-making by authorities and the coastal community.

Supplementary Information The online version contains supplementary material available at https://doi.org/10.1007/s11069-026-08063-3.

Acknowledgements We thank the National Service for Disaster Prevention and Response (SENAPRED) for their insights on coastal risk management, which greatly enriched our analysis. Additionally, we acknowledge María Soledad Tapia, director of the National Fisheries and Aquaculture Service (SERNAPESCA), for support and confidence in our project.

Author contributions Conceptualization: [Catalina Aguirre, Mauricio Molina]; Methodology: [Catalina Aguirre, Mauricio Molina]; Formal analysis and investigation: [Mauricio Molina, Sebastián Correa, Cristian Parra, Sebastián Morales, Daniela Manosalva, Sergio Bahamóndez]; Writing—original draft preparation: [Catalina Aguirre]; Writing—review and editing: [Angella Undurraga]; Funding acquisition: [Gonzalo Concha, Angella Undurraga, Vinka Marincovic, Gisela Irribarra, Catalina Aguirre, Mauricio Molina, Felipe Caselli]; Supervision: [Alejandro de la Maza, Gonzalo Concha, Angella Undurraga].

Funding This work has been supported by Agencia Nacional de Investigación y Desarrollo (ANID). Proyecto FONDEF IDeA I+D 2020 ID20I10404 and IDeA de Investigación Tecnológica 2024 IT24|0160. CA is supported by FONDAP/ANID 1523A0002.

Declarations

Conflict of interests The authors have no relevant financial or non-financial interests to disclose.

References

Aguirre C, Becerra D, Godoy M, Silva D (2020) Interannual variability of ocean surface waves in the Southeast Pacific. EGU General Assembly 2020, 4–8 May. EGU2020-11567. https://doi.org/10.5194/egusphere-egu2020-11567

Aguirre C, Rutllant J, Falvey M (2017) Wind waves climatology of the Southeast Pacific Ocean. Int. J. Climatol. 37(12). https://doi.org/10.1002/joc.5084

Albrecht F, Shaffer G (2016) Regional sea-level change along the Chilean coast in the 21st century. J Coast Res 32(6):1322–1332. https://doi.org/10.2112/jcoastres-d-15-00192.1

Ardhuin F, Rogers E, Babanin A, Filipot J, Magne R, Roland A, Van der Westhuysen A, Queffeulou P, Lefevre J, Aouf L, Collard F (2010) Semiempirical dissipation source functions for ocean waves. Part I: Definition, calibration, and validation. J. Phys. Oceanogr. 40(9). https://doi.org/10.1175/2010JPO4324.1

Bahamóndez S, Aguirre C (2023) Sistema de simulación numérica para la costa de Chile central mediante el acoplamiento de modelos numéricos. Obras Proy. https://doi.org/10.21703/0718-281320233302

Battjes J (1974) Surf Similarity. Coastal Engineering Proceedings, 1 (14): 466–480 https://doi.org/10.9753/icce.v14.26

Beyá J, Álvarez M, Gallardo A, Hidalgo H, Aguirre C, Valdivia J, Parra C, Méndez L, Contreras F, Winckler P, Molina M (2016). Atlas de Oleaje de Chile. Primera edición. Valparaíso, Chile https://oleaje.uv.cl/

Beyá J, Álvarez M, Gallardo A, Hidalgo H, Winckler P (2017) Generation and validation of the Chilean Wave Atlas database. Ocean. Model. 116. https://doi.org/10.1016/j.ocemod.2017.06.004

Camus P, Tomás A, Díaz-Hernández G, Rodríguez B, Izaguirre C, Losada IJ (2019) Probabilistic assessment of port operation downtimes under climate change. Coast Eng 147:12–24. https://doi.org/10.1016/j.coastaleng.2019.01.007

Carvajal M, Contreras-López M, Winckler P, Sepúlveda I (2017) Meteotsunamis occurring along the southwest coast of South America during an intense storm. Pure Appl Geophys 174:3313–3323. https://doi.org/10.1007/s00024-017-1584-0

Carvajal M, Winckler P, Garreaud R, Igualt F, Contreras-López M, Averil P, Cisternas M, Gubler A, Breuer W (2021) Extreme sea levels at Rapa Nui (Easter Island) during intense atmospheric rivers. Nat Hazards 106:1619–1637. https://doi.org/10.1007/s11069-020-04462-2

Cavaleri L, Alves J-HGM, Ardhuin F, Babanin A, Banner M, Belibassakis K, Benoit M, Donelan M, Groeneweg J, Herbers THC, Hwang P, Janssen PAEM, Janssen T, Lavrenov IV, Magne R, Monbaliu J, Onorato M, Polnikov V, Resio D, Rogers WE, Sheremet A, McKee Smith J, Tolman HL, van Vledder G, Wolf J, Young I (2007) Wave modelling – The state of the art. Prog Oceanogr 75:4. https://doi.org/10.1016/j.pocean.2007.05.005

Chawla A, Tolman HL (2007) Automated grid generation for WAVEWATCH III. NOAA National Centers for Environmental Prediction.

Correa S, Aguirre C, Becerra D, Molina M, Vilches P, Bahamóndez S (2025) Upgrade of the Chilean Wave Atlas database. Ocean Model. 193. https://doi.org/10.1016/j.ocemod.2024.102456
Domínguez J, Cienfuegos R, Catalán P, Zamorano L, Lucero F (2014) Assessment of fast spectral wave transfer methodologies from deep to shallow waters in the framework of energy resource quantification in the Chilean coast. Coast. Eng. Proc. 1(34):waves.23. https://doi.org/10.9753/icce.v34.waves.23
Gallardo A, Parra J, Beyá J (2017) Uncertainty of wave extreme values in Chile. Lat Am J Aquat Res 45:4. https://doi.org/10.3856/vol45-issue4-fulltext-2
Guza R, Thornton E, Holman R (1984) Swash on steep and shallow beaches, paper presented at 19th Coastal Engineering Conference, Am. Soc. of Civ. Eng., Houston, Tex.
Harley M, Kinsela M (2022) CoastSnap: a global citizen science program to monitor changing coastlines. Cont Shelf Res 245:104796. https://doi.org/10.1016/j.csr.2022.104796
Hasselmann S, Hasselmann K, Allender J, Barnett T (1985) Computations and parametrizations of the nonlinear energy transfer in a gravity-wave spectrum. Part II: Parametrizations for applications in wave models. J Phys Oceanogr 15:1378–1391. https://doi.org/10.1175/1520-0485(1985)015%3c1378:CAPOTN%3e2.0.CO;2
Heck N, Beck M, Reguero B (2021) Storm risk and marine fisheries: a global assessment. Mar Policy 132:104698. https://doi.org/10.1016/j.marpol.2021.104698
Hemer M, Fan Y, Mori N, Semedo A, Wang X (2013) Projected changes in wave climate from a multi-model ensemble. Nat Clim Change 3:471–476. https://doi.org/10.1038/nclimate1791
Holthuijsen LH, Booij N, Ris R (1993) A spectral wave model for the coastal zone. In: 2nd International Symposium on Ocean Wave Measurement and Analysis, New Orleans, Louisiana, 25–28 July 1993. pp. 630–641.
IPCC (2012) Managing the risks of extreme events and disasters to advance climate change adaptation. A Special Report of Working Groups I and II of the Intergovernmental Panel on Climate Change. Cambridge University Press, Cambridge and New York, 582 pp.
Iribarren R, Nogales C (1949) Protection des ports. Proceedings XVIIth International Navigation Congress, Section II, Communication, vol. 4, Lisbon, pp. 31–80
Koks E, Le Bars D, Essenfelder A, Nirandjan S, Sayers P (2022) The impacts of coastal flooding and sea-level rise on critical infrastructure: a novel storyline approach. Sustain Resil Infrastruct 8(sup1):237–261. https://doi.org/10.1080/23789689.2022.2142741
Liu J, Meucci A, Liu Q, Babanin A, Ierodiaconou D, Young I (2022) The wave climate of Bass Strait and south-east Australia. Ocean Modelling, 172. https://doi.org/10.1016/j.ocemod.2022.101980
Liu Q, Babanin A, Rogers E, Zieger S, Young I, Bidlot J et al., (2021) Global wave hindcasts using the observation-based source terms: Description and validation. Journal of Advances in Modeling Earth Systems, 13(8). https://doi.org/10.1029/2021MS002493
Martínez C, Contreras-López M, Winckler P, Hidalgo H, Godoy E, Agrendano R (2018) Coastal erosion in central Chile: a new hazard? Ocean Coast Manage 156:141–155. https://doi.org/10.1016/j.ocecoaman.2017.07.011
Martínez C, Winckler P, Martín R, Acuña C, Torres I, Contreras-López M (2022) Coastal erosion in sandy beaches along a tectonically active coast: the Chile study case. Prog Phys Geogr Earth Environ 46(2):250–271. https://doi.org/10.1177/03091333211057194
Meucci A, Young I, Hemer M, Kirezci E, Ranasinghe R (2020) Projected 21st-century changes in extreme wind-wave events. Sci. Adv. 6:eaaz7295. https://doi.org/10.1126/sciadv.aaz7295
Morim J, Hemer M, Cartwright N, Strauss D, Andutta F (2018) On the concordance of 21st-century wind-wave climate projections. Glob Planet Change 167:160–171. https://doi.org/10.1016/j.gloplacha.2018.05.005
Morim J, Wahl T, Vitousek S, Santamaria-Aguilar S, Young I, Hemer M (2023) Understanding uncertainties in contemporary and future extreme wave events for broad-scale impact and adaptation planning. Sci Adv. https://doi.org/10.1126/sciadv.ade3170
National Centers for Environmental Prediction (2004) The GFS atmospheric model. Office Note 442. https://repository.library.noaa.gov/view/noaa/11406
Owen, M. W. 1980 Design of seawalls allowing for wave overtopping. HR Wallingford, Report EX 924.
Pawlowicz R, Beardsley B, Lentz S (2002) Classical tidal harmonic analysis including error estimates in MATLAB using T_TIDE. Comput Geosci 28(8):929–937. https://doi.org/10.1016/S0098-3004(02)00013-4
Roberts K, Pringle W, Westerink J (2019) OceanMesh2D 1.0: MATLAB-based software for two-dimensional unstructured mesh generation in coastal ocean modeling. Geosci Model Dev 12:1847–1868. https://doi.org/10.5194/gmd-12-1847-2019
Ruggiero P, Holman R, Beach R (2004) Wave run-up on a high-energy dissipative beach. J Geophys Res Oceans 109:C06025. https://doi.org/10.1029/2003JC002160

Ruggiero P, Komar P, McDougal W, Marra J, Reggie A (2001) Wave runup, extreme water levels and the erosion of properties backing beaches. J Coast Res 17(2):407–419
Stopa J, Cheung K (2014) Intercomparison of wind and wave data from the ECMWF Reanalysis Interim and the NCEP Climate Forecast System Reanalysis. Ocean Model. https://doi.org/10.1016/j.ocemod.2013.12.006
Tolman HL (2002) Alleviating the garden sprinkler effect in wind-wave models. Ocean Model 4:269–289. https://doi.org/10.1016/S1463-5003(02)00004-5
Tolman HL, WAVEWATCH Development Group (2014) User manual and system documentation of WAVEWATCH III version 4.18. NOAA/NWS/NCEP/MMAB Technical Note.
Winckler P, Aguirre C, Farías L, Contreras-López M, Masotti I (2020) Evidence of climate-driven changes on atmospheric, hydrological, and oceanographic variables along the Chilean coastal zone. Clim Change 163:633–652. https://doi.org/10.1007/s10584-020-02805-3
Winckler P, Contreras-López M, Beyá J, Molina M (2017) El temporal del 8 de agosto de 2015 en la región de Valparaíso, Chile central. Lat. Am. J. Aquat. Res. 45(2). https://doi.org/10.3856/vol45-issue4-fulltext-1
Winckler P, Correa S, Garreaud R, Carvajal M (2025) The late December 2024 North Pacific swells on South American coasts. Nat Hazards 121:14487–14511. https://doi.org/10.1007/s11069-025-07366-1
WMO (2022) Early warnings for all: The UN Global Early Warning Initiative for the implementation of climate adaptation. Executive Action Plan 2023–2027. https://library.wmo.int/records/item/58209-early-warnings-for-all (accessed 12 March 2025)
Young I, Ribal A (2019) Multiplatform evaluation of global trends in wind speed and wave height. Science 364:548–552. https://doi.org/10.1126/science.aav9527
Young I, Zieger S, Babanin A (2011) Global trends in wind speed and wave height. Science 332:451–455. https://doi.org/10.1126/science.1197219

Authors and Affiliations

Catalina Aguirre[1,2,3] · Mauricio Molina[1,9] · Sebastián Correa[1] · Daniela Manosalva[1] · Felipe Caselli[1] · Cristian Parra[4] · Sergio Bahamóndez[1,5] · Gonzalo Concha[6] · Angella Undurraga[6] · Alejandro de la Maza[6] · Sebastián Morales[7] · Vinka Marinkovic[8] · Gisela Irribarra[8]

✉ Catalina Aguirre
catalina.aguirre@uv.cl

[1] Escuela de Ingeniería Oceánica, Universidad de Valparaíso, Valparaíso, Chile

[2] Center for Climate and Resilience Research, Santiago, Chile

[3] Centro de Observación y Análisis del Océano Costero, Universidad de Valparaíso, Valparaíso, Chile

[4] Scafom-Rux Chile, Santiago, Chile

[5] Departamento de Geofísica, Universidad de Concepción, Concepción, Chile

[6] Servicio Meteorológico (SERVIMET), Armada de Chile, Valparaíso, Chile

[7] Centro Meteorológico, Armada de Chile, Valparaíso, Chile

[8] Servicio Nacional de Pesca y Acuicultura (SERNAPESCA), Valparaíso, Chile

[9] M5 Data Tech, Puerto Montt, Chile